Surface Review and Letters, Vol. 10, No. 6 (2003) 925–932
© World Scientific Publishing Company

World Scientific
www.worldscientific.com

STUDY OF THE C_2H_4/Si(100)-(2 × 1) INTERFACE BY DERIVATIVE PHOTOELECTRON HOLOGRAPHY

S. H. XU and H. S. WU*
Department of Physics, The University of Hong Kong, Hong Kong, China
**hswu@hkusub.hku.hk*

S. Y. TONG
Department of Physics and Materials Science,
City University of Hong Kong, Hong Kong, China

M. KEEFFE and G. J. LAPEYRE
Physics Department, Montana State University,
Bozeman, MT 59717, USA

E. ROTENBERG
Advanced Light Source, LBNL, Berkeley, CA 94720, USA

Received 5 July 2003

The k derivative spectra (KDS) transform is used for construction of the three-dimensional atomic structure of the C_2H_4/Si(100)-(2 × 1) system from photoelectron diffraction data. The image function obtained by the KDS transform clearly observes the second-layer Si atoms and the C emitters apart from the first-layer Si atoms. The observations of the second-layer Si atoms and the C emitters make it easy to measure the C–C bond length correctly. Then a conclusive adsorption model — the di-σ model — for the C_2H_4/Si(100)-(2 × 1) system is established. In comparison with the KDS transform, the normal small-cone transform hardly measures the C–C bond length. The ability to observe more scatterers of a photoelectron emitter by the KDS transform expands the applicability of holographic imaging.

Keywords: Photoelectron holography; surface structure.

In the past several years, techniques such as photoelectron holographic imaging (PHI),[1–6] low-energy electron diffraction (LEED), Patterson inversion[7,8] and LEED holographic imaging[9,10] have achieved great success in determining 3D atomic structures on clean and adsorbate surfaces. No model calculations were used in the determination of the atomic structures in these techniques. In particular, PHI is appealing because it directly gives positions of scatterers neighboring the selected emitter. Frequently the strong peaks in the images obtained by PHI are only the nearest neighboring atoms around the emitters. The intensities of the peaks corresponding to the scatterers in the image decrease as the distances between the emitter and the scatterers increase. Finally, the peaks for real scatterers vanish while the artifacts prevail in the image. Sometimes, the artifacts are stronger than the peaks corresponding to scatterers. As a result, the correct determination of 3D structure from the image may be difficult, especially for the system whose emitters are at different sites. Recently, we have introduced a new

*Author to whom correspondence should be addressed.

transform, the k derivative spectra (KDS) transform, which produces peaks in the image at greater distances from the emitter.[11] In the present paper, we use the KDS transform to obtain the images for the C_2H_4/Si(100)-(2×1) interface.

An understanding of the bonding of the ethylene molecule provides a foundation for grasping the adsorption behavior of complex unsaturated organic molecules on Si surfaces.[12] Such an interface is also important in the science of silicon carbide formation. The adsorption site for ethylene on the Si(100)-(2×1) surface has been reported based on the results of high-resolution electron energy loss spectroscopy (HREELS) and LEED,[13,14] photoemission spectroscopy (PES),[15,16] PHI,[5] photoelectron diffraction,[17] and scanning tunneling microscopy (STM).[18] All of these studies suggested that ethylene adsorbs on the bridge site and bonds to the dangling bond of two surface silicon atoms. This model is often referred to as the di-σ model, which is shown in Fig. 1. In our recent paper,[5] the normal small-cone transform observed the first-layer Si atoms (A and B), which supports the previous di-σ model. However, the image did not observe the second-layer atoms (C, D, E and F). As discussed later, observation of only the first-layer Si atoms is not enough to construct the adsorption model correctly and straightforwardly. In order to observe more Si atoms, the KDS transform is used. In a surprising success, the KDS transform observes not only the first-layer Si atoms but also the second-layer Si atoms and even the carbon emitters themselves. The observation of the second-layer Si atoms and the carbon emitters makes it easy to construct the adsorption model.

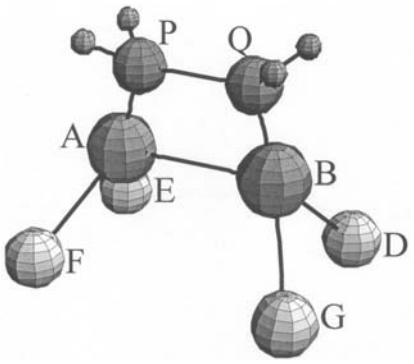

Fig. 1. Ball-and-stick sketches of the Si(100) adsorption sites for ethylene. Big green balls — C atoms P and Q; orange balls — first-layer Si atoms A and B; pink balls — second-layer Si atoms D, E, F and G. The small green balls have been added in the likely positions for the H atoms.

Both the normal small-cone and KDS transforms use angle-resolved photoemission data for the core level of interest. Since the initial energy for the core level is a constant, the resultant spectrum is a constant-initial-energy spectrum (CIS).[19] For each angle the intensity of the emission is measured as a function of wave number k (photon energy). The angles used are uniformly distributed over the emission hemisphere.

Before the transform, a background, $I_0(k)$, is separated from the CIS, $I(k)$. The diffractive portion of the experimental spectrum is extracted using $\chi(k) = I(k)/I_0(k) - 1$. Then two transforms are used to obtain the image function. One transform is the normal inversion with the small-cone technique:[2]

$$U(\mathbf{R}) = \left| \sum_{\hat{k} \in \text{ Cone}(-\mathbf{R}, w)} \int_{k_{\min}}^{k_{\max}} \chi(\mathbf{k}) e^{-ikR(1-\mathbf{k}\cdot\mathbf{R})} d\mathbf{k} \right|^2 . \tag{1}$$

Another transform is KDS inversion which uses the derivative of function χ with respect to the wave number k instead of χ in Eq. (1):[11]

$$U^d(\mathbf{R}) = \left| \sum_{\hat{k} \in \text{ Cone}(-\mathbf{R}, w)} \int_{k_{\min}}^{k_{\max}} \left(\frac{\partial \chi(\mathbf{k})}{\partial k} \right) e^{-ikR(1-\mathbf{k}\cdot\mathbf{R})} d\mathbf{k} \right|^2 . \tag{2}$$

As discussed elsewhere,[2] the sum is over a small cone of width w. The parameter w may range from one spectrum (zero) to all spectra on the hemisphere $(\pi/2)$. Usually a value of around 30° yields an image with minimum artifacts that do not correspond to real atoms.

A theoretical approach[11] has shown that the image function, $U^d(\mathbf{R})$, is related to $U(\mathbf{R})$ through the relationship $U^d(\mathbf{R}) \sim R^2 U(\mathbf{R})$, when there is a real atom at $\mathbf{R}$. In this case, the intensity of the image function is enhanced by the square of the distance between the emitter and the scatterer, R. However, the relationship is not valid if there is no real atom at $\mathbf{R}$. That is to say, the new image function, $U^d(\mathbf{R})$, may observe more distant scatterers than the normal small-cone inversion function, $U(\mathbf{R})$, may.

KDS inversions for several experimental PHD data sets as well as simulated PHD data sets have been examined. The KDS transform always obtains more distant scatterers. Here we present only one experimental case: the double-site adsorbate case of C_2H_4/Si(100). Note that due to the phase shift in the electron scattering factor the distance values may be distorted by 2–3 tenths of an angstrom.[2]

The typical clean Si(100) surface is composed of many terraces separated by single-layer steps. As a consequence, adjacent terraces have dimer directions perpendicular to each other, forming a mixed LEED pattern: $2\times1+1\times2$. It is found that a vicinal (100) surface, miscut by $\sim 3.5°$, with double-layer steps, has a single-domain 2×1 LEED pattern.[20] To make the surface simpler, a vicinal Si(100) surface is used in the present study.

The whole experiment was carried out at the undulator beam-line station 7 at the Advanced Light Source, Lawrence Berkeley National Laboratory. All of the C 1s core-level CIS spectra were collected using a spherical grating monochromator and a large hemispherical electron analyzer. A vicinal Si(100) substrate was introduced into the photoemission chamber and outgassed over 24 h at 400°C. Cyclic annealings at 900°C produced a clean and well-ordered surface, showing a single-domain a 2×1 LEED pattern. The research grade ethylene (99.9 mol % purity) was used to dose the sample by a leak valve while the substrate was at room temperature. The covered surface with ethylene still showed a 2×1 structure as checked by LEED. Incident photon energies of 350–600 eV, corresponding to a range in wave number k of $\sim$ 4–9 $Å^{-1}$, were used. A total of 58 CIS's were collected on a grid covering one fourth of the emission hemisphere, which is an irreducible symmetry element of the surface. After data acquisition, each C 1s core-level spectrum was fitted to a Voigt function to obtain the intensity.

Although they sit in two inequivalent sites, two carbon atoms in one ethylene molecule have the same chemical bonding environment. As the result, the two C atoms (emitters) have the same C 1s core-level spectra. That is to say, all of the CIS's contain the contribution of two inequivalent emitters. In addition, the inversion transform always puts the emitters at the origin (0, 0, 0), i.e. the resultant image puts two C atoms at the origin. Now, imagine shifting the carbon balls in Fig. 1, representing the emitting carbon atoms of the atomic model sketch, towards each other along the line joining them, until they coincide. Thus, the separation between scatterers parallel to the C–C bond in the image has a reduction, while the separation between scatterers perpendicular to the C C bond has no reduction. The amount of this reduction equals the C–C bond length.

Therefore, the measurement of the C–C bond length is key to constructing the adsorption model. In addition, each C emitter is the scatterer of another in one ethylene molecule. It is possible to obtain the C–C bond length directly from the image function. Figure 2 presents the horizontal planar cut passing through the C emitter, which is obtained by the KDS transform. The two emitters are at the origin, labeled as a cross. Generally speaking, strong artifacts often appear in the horizontal planar image, obtained by the normal transform, passing the emitters (see later). It is surprising, however, that the artifacts are very weak in the image obtained by the KDS transform. The two strongest spots, Q/P and P/Q, on the X-axis in the image shown in Fig. 2 are formed by two different C emitters — P and Q, respectively.

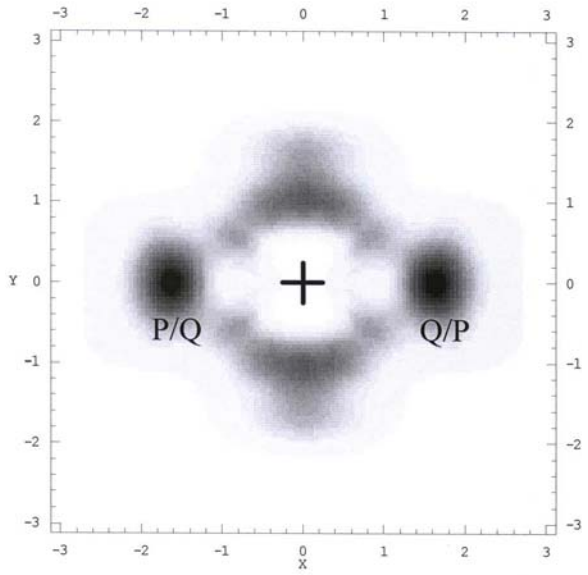

Fig. 2. Horizontal X–Y planar cut from the image function, obtained by the KDS transform, passing through the emitters at $Z = 0.0$ Å. The image is shown in gray scale. Two C emitters (P, Q) are at the origin, labeled as a cross. P/Q (Q/P) means the image of the C atom of P (Q) formed from another C emitter Q (P). There is no background cut at all in this figure and all other figures.

The definition of the symbol Q/P is that P is the emitter when Q is the scatterer. Other weak spots are not associated with real atoms but artifacts. The separation between the Q/P and P/Q spots is twice the C–C bond length. The C–C bond length is found to be 1.6 Å from Fig. 2. This value is in excellent agreement with the bond length (1.62 ± 0.08 Å) measured by photoelectron diffraction.[17] Also the measured length is a little longer than the bond larger (1.34 Å) of the free ethylene molecule, which hints that the C–C bond is not broken but still intact on the Si(100) surface.

Figure 3(a) demonstrates the vertical planar cut, obtained by the KDS transform, passing through the first-layer Si atoms. To aid in recognizing the individual atoms, the cut is accompanied by a ball-and-stick construction for the image, as shown in Fig. 3(b). The emitters do not see themselves but are located at the origin (0,0,0) of the 3D image. Double peaks, A/P and B/Q, are observed and correspond to the first-layer silicon atoms or the Si dimer at $Z = -1.8$ Å. The A/P (B/Q) means that Si atom A (B) is "seen" by C atom P (Q). To relate to the earlier ball-and-stick model of the atomic structure in Fig. 1, consider that the ball representing the carbon emitters is not one atom but two superimposed carbon atoms. The separation 0.6 Å between double peaks is not an interatomic distance but the difference between the Si–Si dimer bond length and the C–C bond length. So, this value gives 2.2 Å for the Si–Si dimer bond length on the surface, which is in agreement with the Si–Si distance (2.36 ± 0.21 Å) obtained by photoelectron diffraction.[17] This value is also close to 2.23 Å of the Si dimer separation on the clean Si surface. Apparently, the adsorption does not break the Si dimer bond.

In Fig. 3(a), there are two weak peaks appearing at each side of the two strongest peaks, A/P and B/Q. These two weak peaks are probably due to real atoms, too. For example, the weak peak B/P at the right side is due to Si atom B "seen" by C emitter P. The position of the peak B/P is $(1.9, 0, -1.8)$. Then, the separation between peaks A/P and B/P or the Si dimer bond length is 2.2 Å. This value is the same as the sum of the separation of the two strongest peaks (0.6 Å) and the C–C bond length (1.6 Å), which forms a consistency check. However, these two weak peaks are not observed in the image obtained by the normal transform.[5]

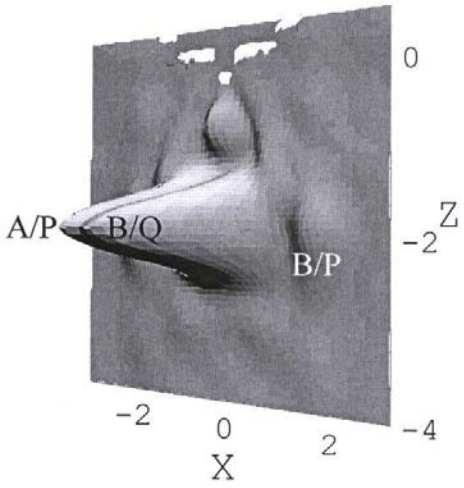

(a)

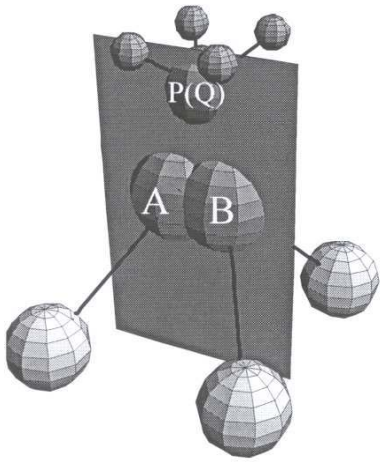

(b)

Fig. 3. (a) Vertical X–Z cut through the chemisorbed ethylene from the image function obtained by the KDS transform. Both carbon emitters are at the origin. The X-axis is the Si–Si dimer direction. Double strong peaks A/P and B/Q are due to Si atom A "seen" by C emitter P and Si atom B "seen" by C emitter Q, respectively. The two weak peaks (the left one is obstructed by the strong peaks) at each side of the strong peaks are probably associated with the real atoms (see text). Another weak peak just below the origin is an artifact. (b) Ball-and-stick construction with a vertical plane that corresponds to the cut shown in (a).

Figures 4(a) and 4(b) show the vertical X–Z planar cut at $Y = 1.92$ Å and the horizontal planar cut at $Z = -2.8$ Å, respectively. Shown in Fig. 4(c) is a ball-stick model with the corresponding planar cuts in order to help understand the images. Two

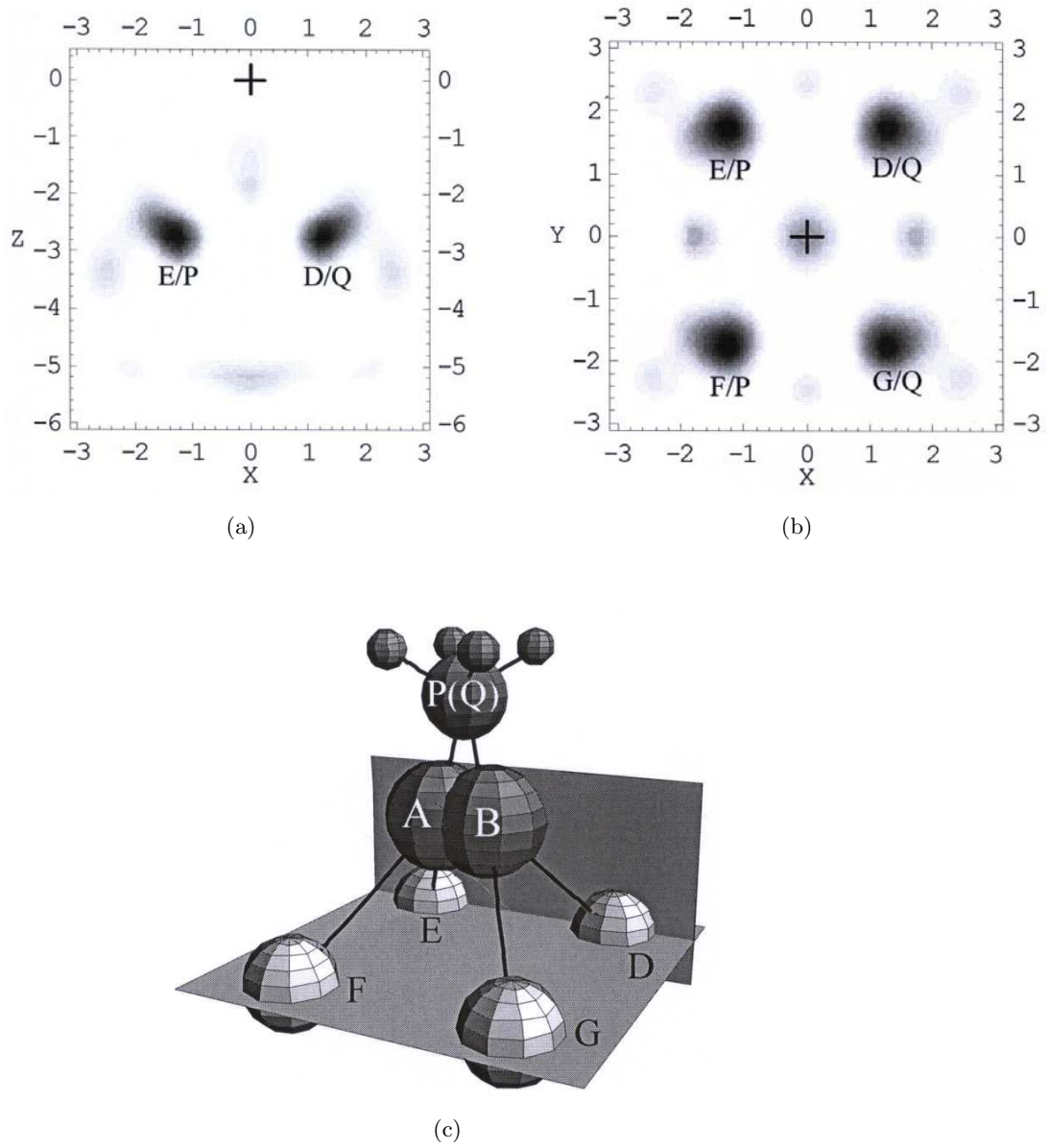

(a) (b)

(c)

Fig. 4. (a) Vertical planar cut at $Y = -1.92$ Å, and (b) horizontal X–Y planar cut at $Z = -2.8$ Å from the image function, obtained by the KDS transform, passing through the second-layer Si atoms. The image is shown in gray scale. The four strongest spots (D/Q, E/P, F/P and G/Q) are observed, which are attributed to the second-layer Si atoms. The other weak spots are due to the artifacts. (c) Ball-and-stick construction with vertical and horizontal planes that are corresponding to the image cuts shown in (a) and (b), respectively.

strongest spots, D/Q and E/P, are found in the vertical planar cut. They are due to the second-layer Si atoms D and E "seen" by the emitters Q and P, respectively. There are four spots (D/Q, E/P, F/P and G/Q) of the highest intensity in the horizontal planar cut. The coordinates of the spot D/Q are $X = 1.2$ Å, $Y = 1.9$ Å and $Z = -2.8$ Å, respectively. As mentioned before, the separation between spot D/Q (G/Q) and spot E/P (F/P) is not the real interatomic distance but the difference between the real interatomic distance and the C–C bond length. Then, a real distance of 4.0 Å between Si atoms D and E is obtained if a C–C bond length of 1.6 Å is used, which agrees well with the bulk value (3.84 Å)

in Si crystal. Conversely, there is no reduction along the Y-axis. The separation (3.8 Å) between spot D/Q (E/P) and G/Q (F/P) in the image is the real interatomic distance. Again, it is very close to the bulk Si–Si distance of 3.84 Å.

From the experimental results shown in Figs. 2–4, we believe that ethylene adsorbs on the bridge site on the Si(100)-(2 × 1) surface. It is in agreement with the di-σ model proposed by the previous research results.[13–18]

In order to demonstrate the advantages of the KDS transform over other transforms, two horizontal planar cuts, obtained by the normal transform, passing the emitters ($Z = 0.0$ Å) and the second-layer Si atoms ($Z = -2.8$ Å), are given in Figs. 5 and 6, respectively. Although two strong spots along the X-axis are found in the image shown in Fig. 5, their intensities are weaker than the artifacts that appear along the Y-axis. Even worse, all the spots of high intensity shown in Fig. 6 are artifacts and cannot be attributed to any of the second-layer Si atoms.

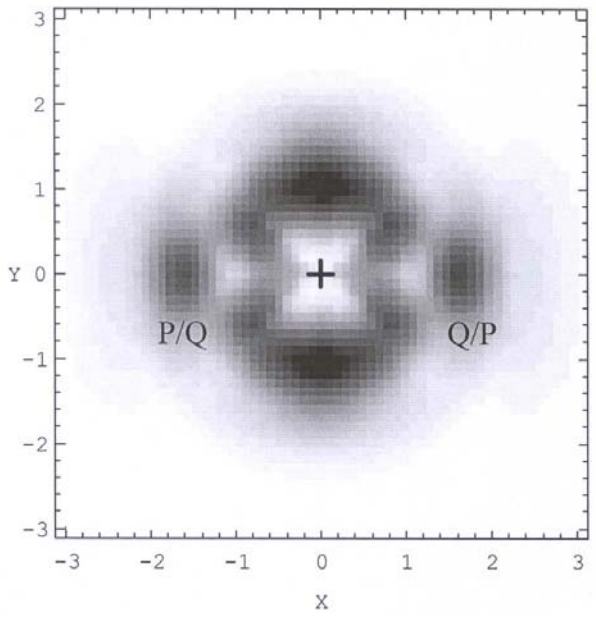

Fig. 5. Horizontal X–Y planar cut from the image function, obtained by the normal small-cone transform, passing through the emitters at $Z = 0.0$ Å. The image is shown in gray scale. P/Q (Q/P) means the image of C atom of P (Q) formed from another C emitter Q (P). Very strong artifacts appear along the Y-axis.

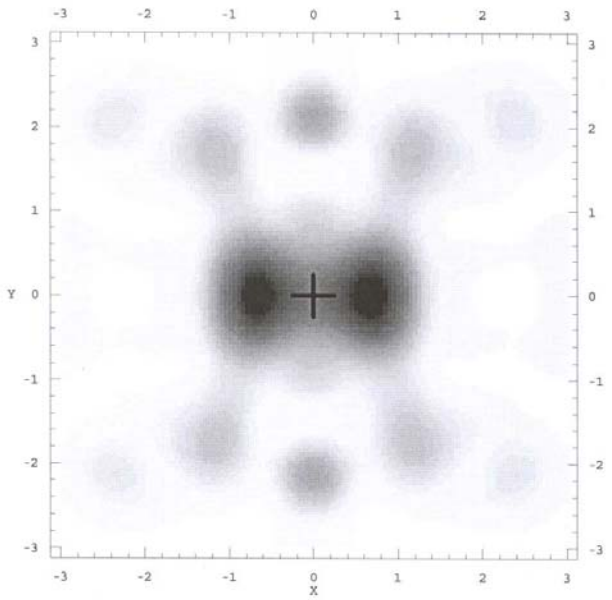

Fig. 6. Horizontal X–Y planar cut from the image function, obtained by the normal transform, passing through the second-layer Si atoms at $Z = -2.8$ Å. The image is shown in gray scale. No obvious strong spots corresponding to the second-layer Si atoms are found except for some artifacts.

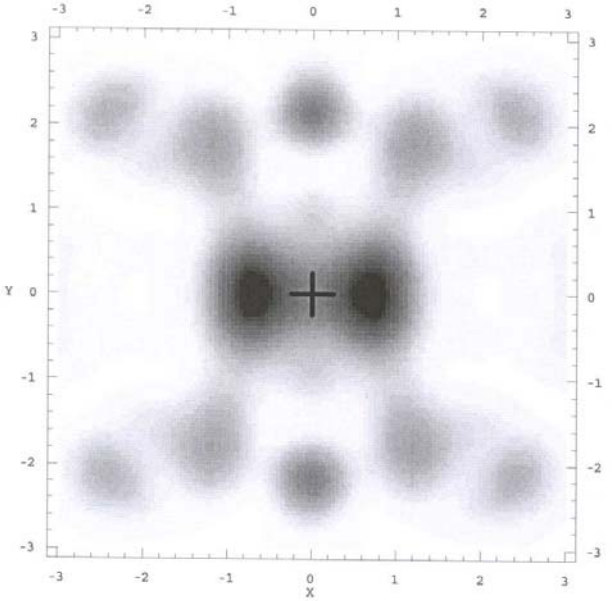

Fig. 7. Horizontal X–Y planar cut from the image function, obtained by the $R^2U(\boldsymbol{R})$ transform, passing through the second-layer Si atoms at $Z = -2.8$ Å. The image is shown in gray scale. No real atoms are found except for some artifacts.

As discussed above, the correct measurement of the C–C bond length is essential for constructing the adsorption model in the present case. However, the C–C bond length can only be obtained from the cuts passing through the C emitters and the second-layer Si atoms. In the normal transform, there is a doubt about obtaining the correct C–C bond length, since the images shown in Figs. 5 and 6 have several strong artifacts. As the result, we do not know the interatomic distance of the first-layer Si atoms. Consequently, the adsorption model cannot be constructed straightforwardly. On the other hand, we can deduce the C–C bond length correctly from the images obtained by the KDS transform. Then, a di-σ adsorption model can be easily constructed.

Now, one may think that the image function will be similar if one the uses $R^2U(\boldsymbol{R})$ transform instead of the KDS transform. As a comparison, Fig. 7 shows the horizontal planar cut at $Z = -2.8$ Å using the $R^2U(\boldsymbol{R})$ transform. It is obvious that Fig. 7 is very different from Fig. 4(b) but similar to the image obtained by the normal transform (Fig. 6). From here we know that the use of the $R^2U(\boldsymbol{R})$ transform cannot increase the power to observe more distant scatterers.

The KDS transform used here is quite different from the self-normalization method proposed by Luh *et al.*[4] Luh *et al.* took the derivative of the PHD data with respect to the photon energy, and then integrated. As expected by Luh *et al.*,[4] this process removed the jumping points or discontinuities that appeared in the PHD data due to the limitations of the experimental condition. In our method, however, we use only the derivative of the function χ, instead of the differentiation–integration cycle. Both the theoretical approach and the images obtained by the KDS transform can truly yield the more distant neighbors (scatterers).

In summary, the KDS transform is used successfully to construct the atomic structures of the experimental system $C_2H_4/Si(100)$-(2×1). The image obtained by the KDS transform can observe not only the first-layer Si atoms but also the second-layer Si atoms and the C emitters, while the image obtained by the normal transform observes only the first-layer Si atoms. The observation of more distant Si atoms makes it more easy and straightforward to construct a correct adsorption model. In addition to the $C_2H_4/Si(100)$-(2×1) interface, the KDS transform has been successfully used for other experimental and simulated PHD data. Therefore, we expect that the KDS transform can be widely used in the clean and adsorbate systems.

Acknowledgments

Research support at Montana State University through NSF Grant No. DMR 9505618 is gratefully acknowledged, as is the support by ONR/DEPSCOR. The authors would like to thank the staff at ALS for their most generous help.

References

1. H. Wu, G. J. Lapeyre, H. Huang and S. Y. Tong, *Phys. Rev. Lett.* **71**, 251 (1993).
2. H.-S Wu and G. J. Lapeyre, *Phys. Rev.* **B51**, 14549 (1995).
3. P. M. Len, J. D. Denlinger, E. Rotenberg, S. D. Kevan, B. P. Tonner, Y. Chen, M. A. Van Hove and C. S. Fadley, *Phys. Rev.* **B59**, 5857 (1999).
4. D.-A. Luh, T. Miller and T.-C. Chiang, *Phys. Rev. Lett.* **81**, 4160 (1998).
5. S. H. Xu, M. Keeffe, Y. Yang, C. Chen, M. Yu, G. J. Lapeyre, E. Rotenberg, J. D. Denlinger and J. T. Yates, Jr., *Phys. Rev. Lett.* **84**, 939 (2000).
6. S. Y. Tong, H. Huang and C. M. Wei, *Phys. Rev.* **B46**, 2452 (1992).
7. H.-S. Wu and S. Y. Tong, *Phys. Rev. Lett.* **87**, 36101 (2001).
8. C. Y. Chang, Z. C. Lin, Y. C. Chou and C. M. Wei, *Phys. Rev. Lett.* **83**, 2580 (1999).
9. M. A. Mendez, C. Glück J. Guerrero, P. L. de Andres, K. Heinz, D. K. Saldin and J. B. Pendry, *Phys. Rev.* **B45**, 9402 (1992).
10. K. Reuter, J. Schardt, J. Bernhardt, H. Wedler, U. Starke and K. Heinz, *Phys. Rev.* **B58**, 10806 (1998).
11. S. H. Xu, H. S. Wu, M. Keeffee, Y. Yang, H. Cruguel and G. J. Lapeyre, *Phys. Rev. B* (in publication).
12. J. T. Yates, Jr., *Science* **279**, 335 (1998).
13. J. Yoshinobu, H. Tsuda, M. Onchi and M. Nishijima, *J. Chem. Phys.* **87**, 7332 (1987).
14. W. Widdra, C. Huang, S. I. Yi and W. H. Weinberg, *J. Chem. Phys.* **105**, 5605 (1996).
15. M. P. Casaletto, R. Zanoni, M. Carbone, M. N. Piancastelli, L. Aballe, K. Weiss and H. Horn, *Phys. Rev.* **B62**, 17128 (2000).
16. W. Widdra, A. Fink, S. Gokhale, P. Trischberger, D. Menzel, U. Birkenheuer, U. Gutdeutsch and N. Rösch, *Phys. Rev. Lett.* **80**, 4269 (1998).
17. P. Baumgärtel, R. Lindsay, O. Schaff, T. Gießbel, R. Terborg, J. T. Hoeft, M. Polcik, A. M. Bradshaw, M. Carbone, M. N. Piancastelli, R. Zanoni, R. L. Toomes and D. P. Woodruff, *New J. Phys.* **1**, 20 (1999).

18. A. J. Mayne, A. R. Avery, J. Knall, T. S. Jones, G. D. A. Briggs and W. H. Weinberg, *Surf. Sci.* **284**, 247 (1993).
19. G. J. Lapeyre *et al.*, *Solid State Commun.* **15**, 1601 (1974).
20. D. E. Aspnes and J. Ihm, *Phys. Rev. Lett.* **57**, 3054 (1986).